AGU PUBLICATIONS

Radio Science

RESEARCH ARTICLE

10.1002/2017RS006283

Key Points:
- Range-resolved incoherent scatter gyrolines seen at Arecibo
- Conventional incoherent scatter theory predicts line shapes
- Widely quoted approximation for gyroline dispersion relation is not generally correct

Correspondence to:
D. L. Hysell,
dlh37@cornell.edu

Citation:
Hysell, D. L., J. Vierinen, and M. P. Sultzer (2017), On the theory of the incoherent scatter gyrolines, *Radio Sci.*, *52*, 723–730, doi:10.1002/2017RS006283.

Received 23 FEB 2017
Accepted 15 MAY 2017
Accepted article online 17 MAY 2017
Published online 1 JUN 2017

On the theory of the incoherent scatter gyrolines

D. L. Hysell[1], J. Vierinen[2], and M. P. Sulzer[3]

[1]Earth and Atmospheric Sciences, Cornell University, Ithaca, New York, USA, [2] Department of Physics and Technology, University of Tromsø, Tromsø, Norway, [3]Arecibo Radio Observatory, Arecibo, Puerto Rico

Abstract The incoherent scatter spectrum feature referred to as the "gyroline" is investigated theoretically and experimentally. The gyroline is associated with the dispersion relation for electrostatic whistler waves. Earlier treatments by Trulsen and Bjørna (1978, and references therein) derive the frequency and growth rate for these waves, but their derivation is only accurate for very small magnetic aspect angles, i.e., for wave vectors close to perpendicular to the geomagnetic field. Their expression for the frequency has the form of a low-order Padé approximate, but we find that a simple formula of this kind accurate for arbitrary magnetic aspect angles does not exist. We therefore analyze the incoherent scatter gyroline feature computationally. The analysis is supported by range-resolved incoherent scatter spectrograms measured recently at Arecibo. The gyroline feature is shown to be strongest in the midlatitude *E* and valley regions where the electron temperature is low enough to avoid cyclotron damping.

1. Introduction

The incoherent scatter radar (ISR) technique is one of the most incisive methods for investigating the ionosphere from the ground. Incoherent scatter arises from thermal fluctuations in a plasma. The shape of the incoherent scatter spectrum is controlled by the dispersion relation for electrostatic plasma waves at the scattering Doppler frequency and wave number. The shape of the so-called "ion line" feature is controlled by the dispersion relation for ion-acoustic waves, and the shape of the "plasma line" feature is controlled by the dispersion relation for Langmuir waves. Information about state parameters of the plasma can be recovered from the characteristics of the spectrum. The theory of incoherent scatter was developed independently by a number of investigators working in parallel [*Salpeter*, 1960; *Fejer*, 1960; *Dougherty and Farley*, 1960; *Farley et al.*, 1961; *Fejer*, 1961; *Hagfors*, 1961; *Salpeter*, 1961; *Rosenbluth and Rostocker*, 1962; *Dougherty and Farley*, 1963; *Perkins et al.*, 1965; *Woodman*, 1967]. Reviews of the theory have been published by *Evans* [1969], *Sheffield* [1975], *Kudeki and Milla* [2011], and *Milla and Kudeki* [2011], among others. *Kudeki and Milla* [2011] and *Milla and Kudeki* [2011] also extended the theory in the case of small magnetic aspect angles.

The geomagnetic field influences the shape of the incoherent scatter spectrum and creates a third spectral feature or line, the "gyroline," which has a shape controlled by the dispersion relation for electrostatic whistler waves. The gyroline feature is weak and generally requires relatively long incoherent integration times to measure. Measurements were performed first at Arecibo by *Behnke and Hagen* [1978] and later at the European Incoherent Scatter (EISCAT) VHF radar by *Bjørna et al.* [1990]. Theory suggested that the gyrolines should be enhanced by resonant suprathermal electrons much as are the plasma lines [*Malnes and Bjørna*, 1993]. Subsequent experiments at EISCAT [*Malnes et al.*, 1993] and Arecibo [*Bhatt et al.*, 2006] confirmed gyroline enhancement by suprathermal electrons although the theoretical details remain to be examined closely.

The theory most often cited to predict the frequency of gyrolines in ISR observations is that of *Trulsen and Bjørna* [1978] and works derived from it. The *Trulsen and Bjørna* [1978] paper itself provides few details about the theoretical derivation but references a pair of technical reports that are not widely available [*Bjørna and Trulsen*, 1976a, 1976b]. Those reports present a detailed derivation of the dispersion relation for Langmuir waves in the presence of a magnetic field (upper hybrid waves) but leave the corresponding analysis of electrostatic whistler waves mainly to the reader and essentially just state the often quoted results. Below, we reconstruct the electrostatic whistler wave theory outlined in the technical reports and argue that it is inappropriate for describing ISR gyroline observations at most geomagnetic latitudes. Alternatives are discussed and evaluated in the context of gyroline spectral measurements from Arecibo.

2. Popular Theory

Electrostatic whistler waves have a frequency given approximately by $\omega \sim \Omega \cos\alpha$, where Ω is the electron gyrofrequency and α is the angle between the wave vector and the geomagnetic field. This familiar fact can be derived using fluid theory and is the starting point for the analysis. Except for wave propagation nearly perpendicular to the magnetic field, ion dynamics would seem to be negligible. The dispersion relation for the waves can be derived from the more accurate standpoint of kinetic theory from the longitudinal projection of the dielectric tensor for electrons taken in the direction of the wave vector **k** [e.g., *Alexandrov et al.*, 1984]

$$\epsilon(\omega, \mathbf{k}) = 1 + \frac{1}{k^2\lambda^2}\left[1 + \sum_{n=-\infty}^{\infty} \frac{\omega}{\sqrt{2}k_\parallel v_t}\Lambda_n(\chi^2)Z(\Theta')\right] \tag{1}$$

where

$$\Lambda_n(\chi^2) \equiv e^{-\chi^2} I_n(\chi^2)$$
$$\chi^2 = \mu \equiv \frac{k_\perp^2 v_t^2}{\Omega^2}$$
$$\Theta' \equiv \frac{\omega - n\Omega}{\sqrt{2}k_\parallel v_t}$$

and where λ is the Debye length, $k_\perp$ and $k_\parallel$ refer to the components of the wave vector perpendicular and parallel to the geomagnetic field, respectively, I_n is the modified Bessel function of the first kind of order n, and $v_t = \sqrt{K_B T/m}$ is the electron thermal speed. The function Z is the plasma dispersion function, the error function of complex argument [*Fried and Conte*, 1961].

In order to simplify the mathematics, *Trulsen and Bjørna* [1978] considered the limiting case:

$$k_\parallel^2 v_t^2 \ll k_\perp^2 v_t^2 \ll \omega^2 \ll \Omega^2 \ll \omega_p^2$$

where ω and ω_p are the wave frequency and plasma frequency, respectively. This implies the consideration of waves propagating close to perpendicular to the geomagnetic field with frequencies well below the electron gyrofrequency. This would appear to be an unsuitable limit for analyzing gyrolines observed at any ISR site other than perhaps Jicamarca. Furthermore, for frequencies well below the electron gyrofrequency, ion dynamics become important, the electrostatic wave in question becomes lower hybrid in nature, and equation (1) by itself is invalid. We moreover expect the gyroline to merge with the ion line and to become indistinguishable as α approaches normal incidence. Consequently, the limit is inappropriate except for waves propagating close to but not too close to perpendicular to the geomagnetic field.

For the sake of completeness, we continue with the derivation in this limit. In the assumed limit, the following parameters can be regarded as being small quantities for purposes of expansion:

$$\frac{k_\perp^2 v_t^2}{\Omega^2} \sim \mathcal{O}(\epsilon)$$
$$\frac{k_\parallel^2 v_t^2}{\omega^2} \sim \mathcal{O}(\epsilon)$$
$$\left|\frac{k_\parallel}{k_\perp}\right| \sim \mathcal{O}(\epsilon)$$

We furthermore make use of the following functional expansions for small μ (with nonnegative or integer n) and large Θ':

$$I_n(\mu) = \left(\frac{1}{2}\mu\right)^n \sum_{k=0}^{\infty} \frac{\left(\frac{1}{4}\mu^2\right)^k}{k!\,\Gamma(n+k+1)} \tag{2}$$

$$Z(\Theta') \approx i\sqrt{\pi}e^{-\Theta'^2} - \Theta'^{-1}\left(1 + \frac{1}{2\Theta'^2} + \frac{3}{4\Theta'^4} + \cdots\right) \tag{3}$$

Consider the dominant $n = 0$ term in equation (1). Making use of the approximations above, the real part of that equation can be expressed as

$$0 = 1 + \frac{\omega_p^2}{k^2 v_t^2}\left[1 - \left(1 - \mu + \frac{3}{4}\mu^2 + \cdots\right)\left(1 + \frac{k_\parallel^2 v_t^2}{\omega^2} + 3\frac{k_\parallel^4 v_t^4}{\omega^4} + \cdots\right)\right] \tag{4}$$

$$\approx 1 + \frac{\omega_p^2}{k^2 v_t^2}\left(\mu - \frac{3}{4}\mu^2\right) - \frac{\omega_p^2}{k^2 v_t^2}\left((1-\mu)\frac{k_\parallel^2 v_t^2}{\omega^2} + 3\frac{k_\parallel^4 v_t^4}{\omega^4}\right) \tag{5}$$

where terms of $\mathcal{O}(\epsilon^2)$ have been retained in equation (5). Next, we recognize $\cos^2\alpha \equiv k_\parallel^2/k^2$. Anticipating the result of the analysis, the ω^4 term above may be replaced with the factor $\omega^2\Omega^2\cos^2\alpha$. Substituting the factors of μ then yields

$$0 = 1 + \frac{\omega_p^2}{k^2 v_t^2}\left(\frac{k_\perp^2 v_t^2}{\Omega^2} - \frac{3}{4}\frac{k_\perp^4 v_t^4}{\Omega^4}\right) - \frac{\omega_p^2}{\omega^2}\left[\cos^2\alpha\left(1 - \frac{k_\perp^2 v_t^2}{\Omega^2}\right) + 3\cos^2\alpha\frac{k^2 v_t^2}{\Omega^2}\right] \tag{6}$$

$$= 1 + \frac{\omega_p^2}{\Omega^2}\left(1 - \frac{3}{4}\frac{k^2 v_t^2}{\Omega^2}\right) - \frac{\omega_p^2}{\omega^2}\cos^2\alpha\left(1 + 2\frac{k^2 v_t^2}{\Omega^2}\right) \tag{7}$$

where the approximation $k_\perp^2 \sim k^2$ has been made in the final analysis, consistent with the limit under consideration.

Finally, we can solve for the frequency of the wave from the resulting quadratic equation.

$$\omega^2 = \frac{\omega_p^2\cos^2\alpha\left(1 + 2\frac{k^2 v_t^2}{\Omega^2}\right)}{1 + \frac{\omega_p^2}{\Omega^2}\left(1 - \frac{3}{4}\frac{k^2 v_t^2}{\Omega^2}\right)} \tag{8}$$

$$= \frac{\Omega^2\cos^2\alpha\left(1 + 2\frac{k^2 v_t^2}{\Omega^2}\right)}{\frac{\Omega^2}{\omega_p^2} + 1 - \frac{3}{4}\frac{k^2 v_t^2}{\Omega^2}} \tag{9}$$

$$\approx \Omega^2\cos^2\alpha\left(1 + \frac{11}{4}\frac{k^2 v_t^2}{\Omega^2} - \frac{\Omega^2}{\omega_p^2}\right) \tag{10}$$

which is the estimate for the real part of the frequency presented by *Trulsen and Bjørna* [1978]. We need only to verify that the $n \neq 0$ terms do not contribute significantly to equation (1). Thisisreadily done, since the next most significant $n = \pm 1$ terms would together contribute to equation (5) in terms only of $\mathcal{O}(\epsilon^3)$ in the limit in question.

To estimate the imaginary part of the wave frequency, define a small imaginary correction term $i\epsilon$ as the product of imaginary part of equation (3) and the terms it multiplies in equation (1):

$$i\epsilon \equiv i\sqrt{\pi}e^{-\Theta'^2}\frac{1}{k^2\lambda^2}\sum_{n=-\infty}^{\infty}\frac{\omega}{\sqrt{2}k_\parallel v_t}\Lambda_n(\chi^2)$$

This correction can be inserted next to the first factor of unity in the denominator of equation (10). Proceeding as before, equation (8) becomes

$$\omega_r^2 + 2i\omega_r\omega_i \approx \Omega^2\cos^2\alpha\left(1 + \frac{11}{4}\frac{k^2 v_t^2}{\Omega^2} - \frac{\Omega^2}{\omega_p^2}\right) + i\epsilon\Omega^2\cos^2\alpha\frac{\Omega^2}{\omega_p^2} \tag{11}$$

Next, a factor of ω_r^2 can be subtracted from each side of equation (11), and with the approximation $\omega_r \approx \Omega\cos\alpha$, the imaginary part of the frequency found by *Trulsen and Bjørna* [1978] can be derived:

$$\omega_i = -\sqrt{\frac{\pi}{8}}\frac{\Omega^4\cos\alpha}{k^3 v_t^3}\sum_{n=-\infty}^{\infty}\Lambda_n(\chi^2)e^{-\Theta'^2} \tag{12}$$

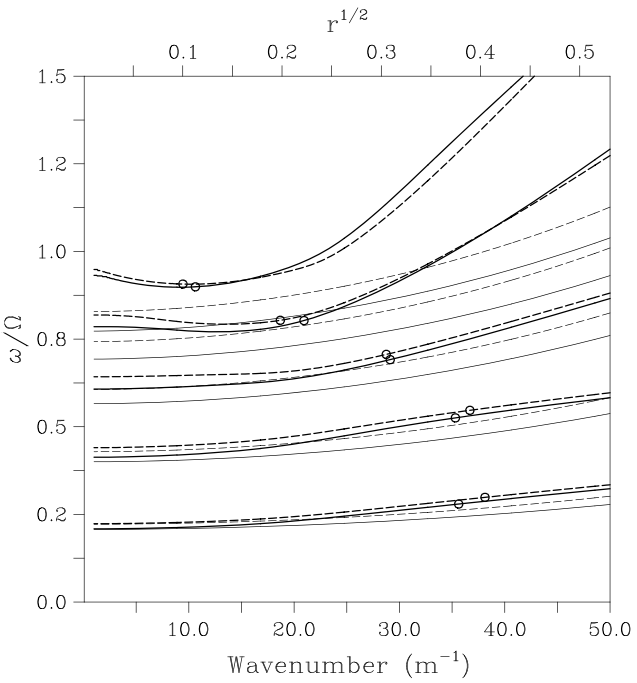

Figure 1. Dispersion relation for electrostatic whistler waves. Five pairs of curves are plotted for angles α of 15, 30, 45, 60, and 75°. Heavy lines represent exact solutions, whereas light lines represent approximations based on equation (9) in the text. The abscissa for the figure is the square root of the parameter $r = k^2 v_t^2/\Omega^2$. The wave number axis has been added for reference taking $T = 700$ K and $\Omega = 2\pi \times 1.5$ MHz. Solid (dashed) lines depict results for $\sqrt{R} = \Omega/\omega_p = 0.75$ (0.6). Circles indicate the highest value of $\sqrt{r}$ for which the damping rate calculated from the exact theory is one tenth the wave frequency.

A numerical solution of equation (1) presents no serious challenges. The dispersion relation can be recast entirely in terms of the dimensionless parameters ω/Ω, Ω/kv_t, and ω_p/kv_t and solved for the first of these given the other two (or some permutation of them—see below) and a fixed specification of α. Furthermore, we can generalize the equation by adding a term for the ions trivially. We can find the roots of the resulting equation using readily available numerical tools. Among these are an efficient plasma dispersion function calculator, a Bessel function evaluator, and a globally convergent optimization method [*Poppe and Wijers*, 1990; *Amos*, 1986; *Powell*, 1970]. The derivatives necessary for calculating the Jacobian matrix have elementary analytic forms.

Figure 1 shows the numerical solutions of the dispersion relation, ions included, for five different angles α. The real part of the wave frequency, normalized to the electron gyrofrequency, is plotted versus the square root of the parameter $r = k^2 v_t^2/\Omega^2$. Curves are plotted for two different values of the square root of the parameter $R = \Omega^2/\omega_p^2$. For reference, a wave number has been added for the special reference case of $T = 700$ K and $\Omega = 2\pi \times 1.5$ MHz. The curves illustrate the complex dependence of the wave frequency on different plasma state parameters. Clearly, the normalized wave frequency is a monotonic function of neither r nor R, in general. Sensitivity to either parameter appears to diminish as the waves approach the low-frequency limit of near-perpendicular propagation.

Also shown in Figure 1 are approximate solutions based on equation (9) in the text. We find first that equation (9) is superior to equation (10) in this instance, the latter relying more heavily on the poorly satisfied approximation $R \ll 1$. Even so, the overall agreement of equation (9) is poor except possibly for the case of $\alpha = 75°$. Only this case satisfies the condition $k_\parallel^2/k_\perp^2 \ll 1$ even passably. Generally and to some degree at all propagation angles, equation (9) underestimates the gyroline frequency, overestimates the sensitivity to changes in R, and fails to capture the complicated dependence on r.

We have calculated but not plotted the imaginary part of the wave frequency as functions of α, r, and R. Instead, the plotter symbols (circles) in Figure 1 indicate the largest value of $\sqrt{r}$ for which the damping rate calculated according to the exact theory is less than one tenth the wave frequency. Damping is due to cyclotron damping which occurs when Θ' is small for some value of n. Since $k_\parallel v_t$ appears in the denominator of Θ', damping is expected to increase with increasing r for given Ω and α. Damping is also most severe for wave frequencies near zero (α approaching 90°) and Ω (α approaching 0°), the former case being less subject to damping because $k_\parallel$ is also identically small. In any case, waves falling to the right of the plotter symbols in Figure 1 may be regarded as being heavily damped and therefore unlikely to be observed in nature absent a source of free energy to destabilize them.

Plasma number density and electron temperature influence the wave frequency and thereby the damping rate. As variations in the number density and temperature push the wave frequency closer to the zeroth or first electron gyroharmonic frequency, damping increases. For waves with frequencies below $\sim \Omega$ and at

most temperatures of interest, the tendency is for frequency to increase with increasing number density and temperature. This implies that increases in number density will tend to increase damping for waves with frequencies approaching but below Ω but decrease it for waves with frequencies much lower than Ω and closer to 0. The plotter symbols in the figure demonstrate this behavior. More important than the effect of changing number density, however, is that of changing temperature, since damping is controlled by the proximity of the frequency and the gyrofrequency compared with the thermal frequency $k_{\|}v_t$. In the lower thermosphere where gyrolines are most readily observed at middle latitudes, the increase in electron temperature with altitude will dominate other concerns in practice and lead to significantly increased damping.

3. Alternative Theory

Obtaining an quantitatively accurate analytic expression for the wave frequency is problematic when $k_{\|}^2/k_{\perp}^2$ is not a small quantity. The main complication arises from the inability to neglect the $n \neq 0$ terms in the summation in equation (1). At the very least, the $n = \pm 1$ terms must be retained, and the $n = \pm 2$ terms contribute to second order when $|k_{\|}/k_{\perp}|$ is no longer small. Moreover, the $n = 1$ term in particular implies a value of Θ' that is only large when the wave frequency differs considerably from the gyrofrequency. This condition is violated generally when the magnetic dip angle is large.

We can note that equation (9) is of the form of a low-order Padé approximate about the origin in a space spanned by the two parameters $r \equiv k^2 v_t^2/\Omega^2$ and $R \equiv \Omega^2/\omega_p^2$. We are therefore motivated to construct an actual Padé approximate for the wave frequency about the point $(r_\circ, R_\circ)$ as

$$\omega^2 = \Omega^2 \cos^2\alpha \frac{a_0 + a_1\left(r - r_\circ\right) + a_2\left(R - R_\circ\right)}{1 + b_1\left(r - r_\circ\right) + b_2\left(R - R_\circ\right)} \tag{13}$$

The five undetermined coefficients are found by equating the numerator of the quotient of equation (13) with the product of the denominator and the first five terms of the Taylor series expansion of $\omega^2/(\Omega^2\cos^2\alpha)$. The coefficients in the Taylor series expansion involve the derivatives of this ratio with respect to r and R which can be estimated numerically from the roots of equation (1) at each point ($r_\circ$ and $R_\circ$) of expansion. This leads to a system of linear equations which can be solved for the five Padé approximation coefficients at each point.

Figure 2 shows the results of such a computation for the case of $\alpha = 45°$. For a given wave number k and gyrofrequency Ω, the variables r and R correspond to the temperature and plasma frequency, respectively. For example, for a 430 MHz radar and an electron gyrofrequency of $\Omega = 2\pi \times 0.87$ MHz, taking $T = 700$ K and $\omega_p = 2\pi \times 2$ MHz implies $r = 0.11$ and $R = 0.19$.

We have verified that equation (13), populated using coefficients from Figure 2, gives a good approximation of the $\alpha = 45°$ curves in Figure 1. The formula may be useful for testing the sensitivity of the gyroline to small variations in state parameters that are essentially well known (from simultaneous ion line or plasma line measurements, for example). However, the domain of convergence of the Padé approximation is limited in view of the rapid variations in a_1 and b_1 and the sensitivity of the shape of the dispersion curve to r in the low-r regime. This sensitivity is most acute for $r \lesssim 0.1$, a domain which encompasses the conditions likely to apply to waves observed in nature. This analysis indicates that deriving an expression similar in form to equation (9) with a wide domain of practical applicability is not possible. While the formula in equation (9) can be nearly reproduced with the right choice of $r_\circ$ and $R_\circ$, the agreement is fortuitous. While a higher-order Padé approximate should give better performance, the complexity of the formula would begin to compete with that of the original problem posed by equation (1) and so would be of questionable utility.

The analysis indicates that deriving an expression similar in form to equation (9) with a wide domain of practical applicability, e.g., in data-model fitting situations, is not possible.

4. Observations

We turn now to some example plasma line and gyroline spectra measured recently at the Arecibo Observatory. The measurements were made at night, from before sunset to after sunrise, between 12 October 2016 22:00 and 13 October 2016 11:00 UTC. We have seen that a theory of the form of equation (13) cannot generally be expected to predict the gyroline frequency. Here we examine whether the more complete theory represented by equation (1) and the theory of incoherent scattering based on it can.

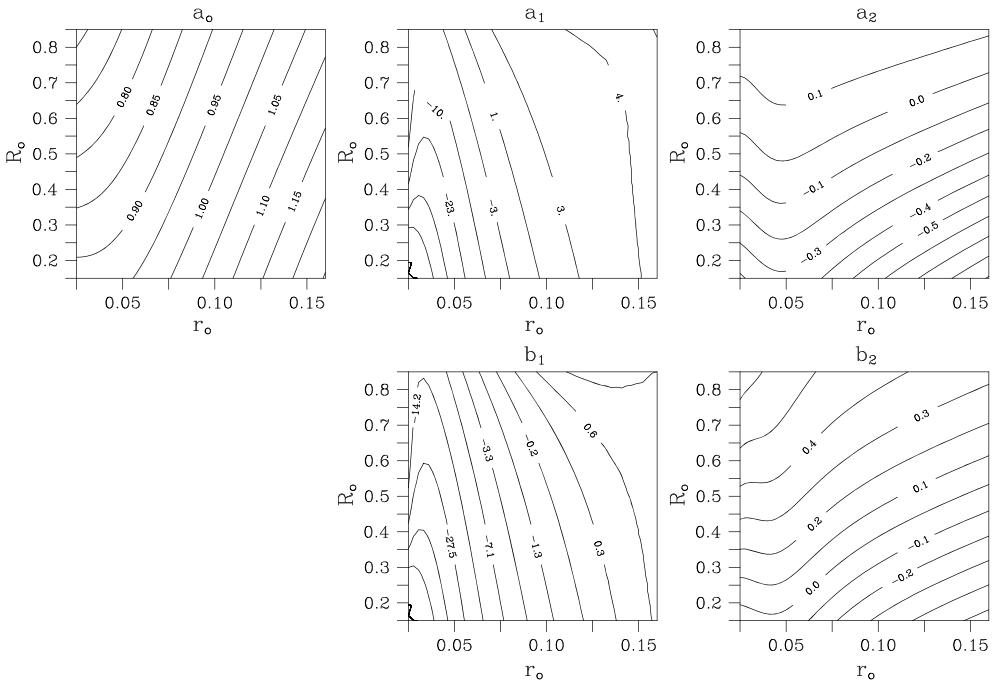

Figure 2. Coefficients for the Padé approximation of the gyroline frequency given by equation (13) versus the expansion parameters r and R. For this figure, $\alpha = 45°$ (see text).

The radar experiment utilized a 440 μs long uncoded pulse with a 10 ms interpulse period and a 440 μs pseudorandom binary phase coded long pulse with 2 μs baud length. The uncoded and coded long pulse experiments were run in 10 s segments. The peak transmit power was around 1 MW. Only the uncoded pulses were used for the gyroline and plasma line in order to avoid self-noise from ion line spreading in Doppler frequency. We used the linefeed antenna pointed in the fixed vertical direction to maximize gain. Data were recorded with a 16 bit complex baseband digital receiver at a 25 MHz sample rate and stored to disk. The gyrolines were analyzed using a power-averaged range-Doppler filter bank on the output of a matched filter output of the uncoded long pulse. The filter bank was implemented with a 22,500-point zero-padded fast Fourier transform. We used a range spacing of 20 μs. To improve the variance of the errors, 25 neighboring frequency bins were averaged together to obtain an effective frequency resolution of 27.8 kHz. The integration time was 10 min which was sufficient to show gyroline and plasma line throughout the experimental period. Due to the cycling between coded and uncoded pulses, the effective integration time for the gyroline observation was 5 min. The ambiguity-convolved averaged range-Doppler measurements were deconvolved using the CLEAN algorithm [*Högbom*, 1974] in a similar manner as was used previously for deconvolution of high time resolution

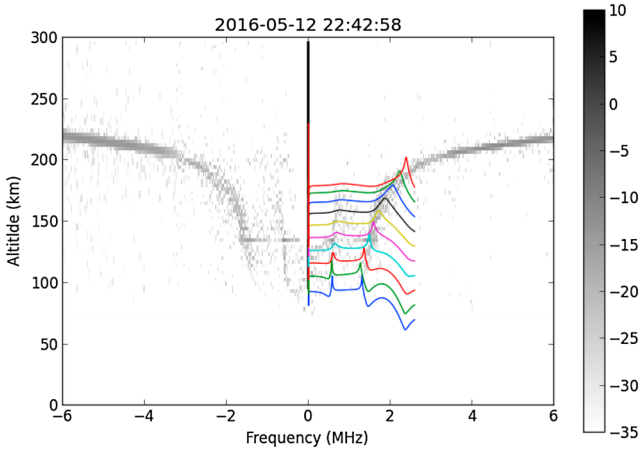

Figure 3. High-bandwidth, range-resolved spectrum acquired at Arecibo on 12 May 2016 at 2242 UT. (LT = UT − 4 h.) Gray scales denote signal-to-noise ratio on a dB scale. Gyroline and plasma line features are clearly visible between 100 and 200 km altitude at frequencies below and above 1 MHz, respectively. Curves representing the theoretical incoherent scatter spectrum for altitudes between 100 and 200 km in 10 km increments are superimposed (see text).

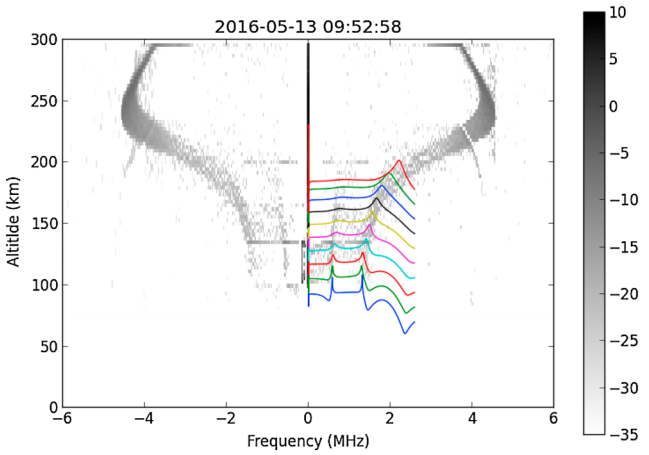

Figure 4. Same as Figure 3 except for 13 May, 0952 UT.

auroral enhancements of plasma lines [*Vierinen et al.*, 2016]. For the ion line, we used the coded long pulse and superposed the ion line to the gyroline and plasma line portion of the echo.

The experiment detected plasma lines and gyrolines in the *E* region and the *F* region bottomside throughout the whole night. A continuum of plasma lines from the *F* region peak down to the gyroline was observed throughout of night. Plasma lines were also observed between the *F* region to and an altitude of up to about 1000 km and a plasma frequency of 1 MHz. No gyrolines were observed in the topside.

Figure 3 shows experimental results for conditions shortly after sunset on 12 May, and Figure 4 shows results around sunrise on 13 May 2016. These are the times when the gyrolines are most distinct although they are observed throughout the night. The upshifted and downshifted plasma and gyrolines are clearly evident in both figures.

We note that the plasma lines in Figure 4 exhibit considerable spectral broadening, particularly between 200 and 250 km altitude. This reflect temporal variations in the ionosphere during the 10 min that data were being acquired. Similar broadening is expected in all of the observations but is most obvious around the time of sunrise. Comparable broadening is absent in the gyroline echoes. This reflects the relative insensitivity of the gyroline frequency to plasma state parameters.

Incoherent scatter spectra for altitudes between 100 and 200 km altitude in 10 km increments are superimposed on the spectrograms. Conventional incoherent scatter theory and numerical analysis was used to generate these spectra [see, e.g., *Farley et al.*, 1961]. In order to set the parameter $r = k^2 v_t^2/\Omega^2$ versus altitude, the International Geomagnetic Reference Field for the current epoch was used (for the magnetic field strength and dip angle) along with the International Reference Ionosphere (IRI-2016) (for T_e) [*Thébault and other*, 2015; *Bilitza et al.*, 2016]. The parameter $R = \Omega^2/\omega_p^2$ was set through a fitting procedure: the parameter $k^2\lambda_d^2$ was parametrized using a second-degree polynomial in the altitude, and the polynomial coefficients were determined through nonlinear least squares fitting. The fitting found the coefficients that maximized the congruence between the theoretical and observed spectra globally at all altitudes considered.

The theory is able to assign mutually consistent plasma line and gyroline frequencies over the altitudes where the former are observed. It also demonstrates the altitude limitations of gyroline detectability. Below about 100 km at night, there is insufficient plasma density for detecting incoherent scatter. At higher altitudes, increasing electron temperature leads to increasing cyclotron damping. The effect is exacerbated slightly by the increase in wave frequency accompanying increases in number density and electron temperature. Above about 200 km, depending on conditions, cyclotron damping essentially eliminates the gyroline resonance.

5. Summary and Conclusion

We have examined the wave equation for the electrostatic whistler waves that underlie the gyroline feature of the incoherent scatter spectrum. Two natural expansion parameters are $r \equiv k^2 v_t^2/\Omega^2$ and $R \equiv \Omega^2/\omega_p^2$. Contrary to earlier work on the problem, we find no elementary analytic expression for the wave frequency and growth rate based on these expansion parameters. That the wave frequency cannot be expressed in terms of a low-order Pade approximate in these parameters in a robust way suggests that no such expression exists.

At Arecibo, the gyroline feature is most prominent in the *E* and valley regions where electrons are abundant and where the electron temperature is relatively low. The latter condition is required to avoid cyclotron damping. More specifically, the requirement is that the difference between the wave frequency and an electron gyroharmonic frequency measured in terms of the thermal frequency should be large. The higher

the geomagnetic latitude of the observations, the more difficult it is to satisfy the condition since the wave frequency approaches the electron gyrofrequency as the dip angle increases.

Testing gyroline theory required the measurement of range-resolved spectrograms. The observations shown in this paper resulted from a conventional long-pulse experiment at Arecibo. Numerical deconvolution of the transmitter waveform from the received signal was used to improve the range resolution of the incoherent scatter spectrograms. The quality of the data thus obtained was adequate for spectral fitting given 5 min effective incoherent integration times (and 10 min total observing times). The sensitivity of the Arecibo observatory was therefore prerequisite for this study.

Acknowledgments
This work was supported by award AGS-1360718 from the National Science Foundation to Cornell University. The Arecibo Observatory is part of the National Astronomy and Ionosphere Center which is operated under a cooperative agreement with the National Science Foundation. Data acquired at the Arecibo Observatory are archived in the Madrigal Database at http://madrigal.naic.edu.

References

Alexandrov, A. F., L. S. Bogdankevich, and A. A. Rukhadze (1984), *Principles of Plasma Electrodynamics*, Springer, New York.
Amos, D. E. (1986), A portable package for Bessel functions of a complex argument and nonnegative order, *Trans. Math. Software*, *12*, 265–273.
Behnke, R. A., and J. B. Hagen (1978), Incoherent scattering of radio waves by whistler mode oscillations in the ionosphere, *Radio Sci.*, *13*, 215–218.
Bhatt, A. N., E. A. G. Kendall, M. C. Kelley, M. P. Sulzer, and E. B. Shume (2006), Observations of strong gyro line spectra at Arecibo near dawn, *Geophys. Res. Lett.*, *33*, L14105, doi:10.1029/2006GL026139.
Bilitza, D., D. Altadill, B. Reinisch, I. Galkin, V. Shubin, and V. Truhlik (2016), *The International Reference Ionosphere: Model Update 2016*, vol. 18, 9671 p., EGU General Assembly Conference Abstracts, Vienna, AT.
Bjørna, N., and J. Trulsen (1976a), Incoherent scattering from thermal fluctuations in a magnetoplasma, *Tech. Rep. 22–76*, The Auroral Obs., Univ. of Tromsø.
Bjørna, N., and J. Trulsen (1976b), Influence of electrostatic electron waves on the differential scattering cross-section, *Tech. Rep. 28–76*, The Auroral Obs., Univ. of Tromsø.
Bjørna, N., B. T. Esjeholm, and T. H. Hansen (1990), Gyro line observations with the EISCAT VHF radar, *J. Atmos. Terr. Phys.*, *52*, 473–482.
Dougherty, J. P., and D. T. Farley (1960), A theory of incoherent scattering of radio waves by a plasma, *Proc. R. Soc*, *A259*, 79–99.
Dougherty, J. P., and D. T. Farley (1963), A theory of incoherent scattering of radio waves by a plasma: 3. Scattering in a partly ionized gas, *J. Geophys. Res.*, *68*, 5473–5486.
Evans, J. V. (1969), Theory and practice of ionosphere study by Thomson scatter radar, *Proc. IEEE*, *57*, 496–530.
Farley, D. T., J. P. Dougherty, and D. W. Barron (1961), A theory of incoherent scattering of radio waves by a plasma: 2. Scattering in a magnetic field, *Proc. R. Soc. London Ser. A*, *263*, 238–258.
Fejer, J. A. (1960), Scattering of radio waves by an ionized gas in thermal equilibrium, *Can. J. Phys.*, *38*, 1114–1133.
Fejer, J. A. (1961), Scattering of radio waves by an ionized gas in thermal equilibrium in the presence of a uniform magnetic field, *Can. J. Phys.*, *39*, 716–740.
Fried, B. D., and S. D. Conte (1961), *The Plasma Dispersion Function and Hilbert Transform of the Gaussian*, Acad. Press, New York.
Hagfors, T. (1961), Density fluctuations in a plasma in a magnetic field, with applications to the ionosphere, *J. Geophys. Res.*, *66*, 1699–1712.
Högbom, J. (1974), Aperture synthesis with a non-regular distribution of interferometer baselines, *Astron. Astrophys. Suppl. Ser.*, *15*, 417–426.
Kudeki, E., and M. Milla (2011), Incoherent scatter spectral theories. Part I: A general framework and results for small magnetic aspect angles, *IEEE Trans. Geosci. Remote Sens.*, *49*(1), 315–328.
Malnes, E., and N. Bjørna (1993), Enhancement of incoherent scatter gyro lines by suprathermal electrons, *J. Atmos. Terr. Phys.*, *55*, 667–674.
Malnes, E., N. Bjørna, and T. L. Hansen (1993), European incoherent scatter VHF measurements of gyrolines, *J. Geophys. Res.*, *98*, 21,563–21,569.
Milla, M., and E. Kudeki (2011), Incoherent scatter spectral theories—Part II: Modeling the spectrum for modes propagating perpendicular to B, *IEEE Trans. Geosci. Remote Sens.*, *49*(1), 329–345.
Perkins, F. W., E. E. Salpeter, and K. O. Yngvesson (1965), Incoherent scatter from plasma oscillations in the ionosphere, *Phys. Rev. Lett.*, *14*, 579–581.
Poppe, G. P. M., and C. M. J. Wijers (1990), More efficient computation of the complex error function, *Trans. Math. Software*, *16*, 38–46.
Powell, M. J. D. (1970), A hybrid method for nonlinear equations, in *Numerical Methods for Nonlinear Algebraic Equations*, edited by P. Rabinowitz, pp. 87–114, Gordon and Breach, London.
Rosenbluth, M. N., and N. Rostocker (1962), Scattering of electromagnetic waves by a nonequilibrium plasma, *Phys. Fluids*, *5*, 776–788.
Salpeter, E. E. (1960), Electron density fluctuations in a plasma, *Phys. Rev.*, *120*, 1528–1535.
Salpeter, E. E. (1961), Plasma density fluctuations in a magnetic field, *Phys. Rev.*, *122*, 1663–1674.
Sheffield, J. (1975), *Plasma Scattering of Electromagnetic Radiation*, Acad. Press, New York.
Thébault, E., and other (2015), International Geomagnetic Reference Field: The 12th generation, *Earth Plantes Space*, *67*, 69, doi:10.1186/s40623-015-0228-9.
Trulsen, J., and N. Bjørna (1978), Influence of electrostatic electron waves on the incoherent scattering cross-section, *Phys. Src.*, *17*, 11–14.
Vierinen, J., A. Bhatt, M. A. Hirsch, A. Strømme, J. L. Semeter, S.-R. Zhang, and P. J. Erickson (2016), High temporal resolution observations of auroral electron density using superthermal electron enhancement of Langmuir waves, *Geophys. Res. Lett.*, *43*, 5979–5987, doi:10.1002/2016GL069283.
Woodman, R. F. (1967), Incoherent scattering of electromagnetic waves by a plasma, PhD thesis, Harvard Univ.